

THE OBLATE SCHWARZSCHILD APPROXIMATION FOR LIGHT CURVES OF RAPIDLY ROTATING NEUTRON STARS

SHARON M. MORSINK^{1,2}, DENIS A. LEAHY³, COIRE CADEAU¹, & JOHN BRAGA¹

Accepted by the Astrophysical Journal

ABSTRACT

We present a simple method for including the oblateness of a rapidly rotating neutron star when fitting X-ray light curves. In previous work we showed that the oblateness induced by rotation at frequencies above 300 Hz produces a geometric effect which needs to be accounted for when modelling light curves to extract constraints on the neutron star's mass and radius. In our model X-rays are emitted from the surface of an oblate neutron star and propagate to the observer along geodesics of the Schwarzschild metric for a spherical neutron star. Doppler effects due to rotation are added in the same manner as in the case of a spherical neutron star. We show that this model captures the most important effects due to the neutron star's rotation. We also explain how the geometric oblateness effect can rival the Doppler effect for some emission geometries.

Subject headings: stars: neutron — stars: rotation — X-ray: binaries — relativity — pulsars: general

1. INTRODUCTION

The observation of pulsed X-ray emission originating from the surfaces of rotating neutron stars provides an excellent opportunity to study the properties of neutron stars and to possibly constrain the equation of state (EOS) of supernuclear density matter. Detailed modelling of the properties of the emitting region on the star combined with relativistic raytracing can be used to create theoretical light curves which can then be compared with the observed light curves to constrain the masses and radii (and hence the EOS) of the X-ray emitting neutron stars.

The best candidates for a pulse-shape analysis are the accreting neutron stars where the energy released from accretion leads to X-ray emission from the surfaces of the neutron stars. The accreting neutron stars that are of interest fall into three classes: slowly rotating X-ray pulsars such as Her X-1; accreting ms-Period neutron stars exhibiting Type I X-ray bursts; and the accreting ms-Period X-ray pulsars such as SAX J1808.4-3658. (These classes are not mutually exclusive: some of the accreting ms pulsars are also Type I bursters.) In the case of Her X-1 (with a spin period of 1.24 s), Leahy (2004) has shown that an accretion-column model can explain the data and constrain the dimensionless mass-to-radius ratio to the range $0.18 \leq M/R \leq 0.19$. Bhattacharyya et al. (2005) modelled the burst oscillations detected during Type I X-ray bursts originating on XTE J1814-338 (spin period 3.2 ms) and found an upper limit of $M/R \leq 0.24$. An analysis of the X-ray pulse shape of SAX J1808.4-3658 (spin period 2.5 ms) by Poutanen & Gierliński (2003) also provided constraints on the mass-to-radius ratios to the range $0.18 \leq M/R \leq 0.3$. In addition, one non-accreting ms X-ray pulsar

PSR J0437-4715 has been modelled by Bogdanov et al. (2006) and has been shown to be consistent with a radius $R > 6.7$ km. While none of these constraints are strong enough to conclusively rule out any equations of state, these studies do show a great deal of promise.

The most commonly used approximation used to model neutron star light curves is the Schwarzschild + Doppler (S+D) approximation (Miller & Lamb 1998; Poutanen & Gierliński 2003). In the S+D approximation the gravitational light-bending effects are modelled as though the star is not rotating using the Schwarzschild metric and the formalism prescribed by Pechenick, Ftaclas, & Cohen (1983). Rotational effects are added by introducing Doppler terms as though the star is a rotating object with no gravitational field. In our previous calculations (Cadeau et al. 2007) we found that as long as the star's spin frequency is below 300 Hz, the ratio M/R can be accurately extracted using the S+D approximation.

In two recent papers (Cadeau et al. 2005, 2007) we investigated the validity of the S+D approximation by computing the geodesics of rapidly rotating neutron stars using the exact numerical metric to describe the gravitational field and the shape of the star. We have shown (Cadeau et al. 2005) that it is necessary to correctly bin the light curve so that the variable times of arrival of photons from different parts of the star are taken into account if the star is rapidly rotating. However, we also showed that it was sufficient to use the Schwarzschild geometry to calculate the times of arrival: the effect of frame-dragging on light-bending and times of arrival is not large enough to affect the light curves, consistent with the calculations done by Braje et al. (2000).

In the second paper (Cadeau et al. 2007) we investigated the effect of the neutron star's oblate shape. Previous calculations (Braje & Romani 2001) of magnetospheric scattering found that the oblate shape of a rotating neutron star can alter the directions that photons are scattered into. In our computations (without scattering) we found that the oblate shape has a significant effect on the light curves which should be included when modelling the light curves of rapidly rotating neutron stars.

¹ Department of Physics, University of Alberta, Edmonton AB, T6G 2G7, Canada

² On sabbatical at: Pacific Institute for Theoretical Physics, Department of Physics and Astronomy, University of British Columbia, 6224 Agricultural Road, Vancouver BC, V6T 1Z1, Canada

³ Department of Physics and Astronomy, University of Calgary, Calgary AB, T2N 1N4, Canada

The reason for the importance of oblateness is simply geometrical: when light is emitted from an oblate surface the directions that the light can be emitted into are different from those possible from the surface of a spherical star. This leads to certain spot locations on the star where the spot is visible if the surface is oblate but would be invisible if the surface were spherical (and vice versa).

In our previous work (Cadeau et al. 2007) we found that as long as the correct shape of the star is used to formulate the initial conditions, the light curves resulting from tracing rays in the Schwarzschild metric are a very good approximation to the light curves resulting from ray-tracing in the full numerical metric of a rapidly rotating neutron star. The problem with the method used in our past work is that it is too slow for use in fitting light curves to theoretical models. In our past work a full relativistic stellar structure calculation as well as geodesics connecting all spot and observer latitudes had to be computed for each hypothetical neutron star model. Since many thousands of models must be computed in order to fit the neutron star's properties to a light curve, our past work was not useful for comparing theoretical calculations with X-ray timing data.

The purpose of this paper is to present a simple approximation that includes the essential features of our more detailed ray-tracing calculations for rapidly rotating neutron stars. Our new approximation, the Oblate Schwarzschild (OS) approximation, is based on the more commonly used S+D approximation. In the OS approximation an empirical formula for the oblate shape of the rotating neutron star is used to define initial conditions and visibility conditions for photons. Once initial conditions on the surface of the star are set up, the Schwarzschild metric is used to find bending angles and photon time delays. Doppler effects due to rotation are then added to the model in the same manner as in the S+D approximation.

The outline of this paper is as follows. In Section 2 we present a simple empirical formula for the shape of the star and derive expressions for the vector normal to the surface, angles between the surface normal and the light rays, and the solid angle subtended by an oblate surface. In Section 3 we explain how these concepts are used to create light curves in the OS approximation, providing details of how the new visibility condition is implemented. In Section 4 we explain why the geometric effect of oblateness can rival the Doppler effect for some emission geometries. In Section 5 we compare our approximate light curves with light curves computed using our previous exact methods. Finally, we conclude with comments on possible applications of the OS approximation.

2. THE OBLATE SHAPE OF A ROTATING NEUTRON STAR

In the OS approximation, an oblate surface is embedded in the metric of a non-rotating neutron star. The metric exterior to a non-rotating neutron star is given by the Schwarzschild solution

$$ds^2 = - \left(1 - \frac{2M}{r}\right) dt^2 + \left(1 - \frac{2M}{r}\right)^{-1} dr^2 + r^2 (d\theta^2 + \sin^2 \theta d\phi^2). \quad (1)$$

(We use gravitational units where $G = c = 1$.) The surface of the star is described by a function $r = R(\theta)$,

and will be specified in subsection 2.1. Given a function describing the surface of the star, the surface area of a small spot of angular extent $d\theta$ and $d\phi$ located at angles θ and ϕ on the surface of the star will have a surface area

$$dS(\theta) = R^2(\theta) \sin \theta (1 + f^2(\theta))^{1/2} d\theta d\phi \quad (2)$$

where the function $f(\theta)$ is defined by

$$f(\theta) = \frac{(1 - 2M/R)^{-1/2} dR}{R} = \frac{(1+z)}{R} \frac{dR}{d\theta}, \quad (3)$$

where the gravitational redshift $z = 1/\sqrt{1 - 2M/R} - 1$ has been introduced.

An alternative (but equivalent) description of the gravitational field exterior to a non-rotating star is given by the Isotropic Schwarzschild metric (see, for example, Misner, Thorne, & Wheeler (1973))

$$ds^2 = - \left(\frac{1 - M/2\bar{r}}{1 + M/2\bar{r}} \right)^2 dt^2 + (1 + M/2\bar{r})^4 (d\bar{r}^2 + \bar{r}^2 (d\theta^2 + \sin^2 \theta d\phi^2)), \quad (4)$$

where the isotropic radial coordinate \bar{r} is related to the areal radial coordinate r by the transformations

$$r = \bar{r} (1 + M/2\bar{r})^2 \quad (5)$$

and

$$dr = (1 - 2M/r)^{1/2} (1 + M/2\bar{r})^2 d\bar{r}. \quad (6)$$

The surface of the star in this coordinate system is denoted $\bar{r} = \bar{R}(\theta)$. Making use of the coordinate transformations given by equations (5) and (6) it is easily shown that the function $f(\theta)$ defined in equation (3) is

$$f(\theta) = \frac{1}{\bar{R}} \frac{d\bar{R}}{d\theta}. \quad (7)$$

2.1. A Model for Oblateness

In order to find the shape of a rotating neutron star, it is necessary to specify an equation of state (EOS) of dense nuclear matter, a spin period and mass and then solve the relativistic equations of stellar structure. The relativistic stellar structure equations must be solved numerically using an axisymmetric code such as `rns`⁴ (Stergioulas & Friedman 1995), based on the methods described by Cook, Shapiro, & Teukolsky (1994). Once the stellar structure equations have been solved, the location of the star's surface is extracted by finding the locations where the fluid's enthalpy vanishes.

In order to aid the process of fitting light curves, we have found a simple empirical formula for the shapes of rotating neutron stars. We assume that the surface of a rotating neutron star can be described by a function of the form

$$\frac{R(\theta)}{R_{eq}} = 1 + \sum_{n=0}^2 a_{2n}(\zeta, \epsilon) P_{2n}(\cos \theta) \quad (8)$$

where θ is the co-latitude, measured from the spin axis ($\cos \theta = 0$ on the equator), $P_n(\cos \theta)$ is the Legendre polynomial of order n , R_{eq} is the radius of the rotating

⁴ Available at <http://www.gravity.phys.uwm.edu/rns>

star measured at the equator and the parameters ζ and ϵ are given by

$$\zeta = \frac{GM}{R_{eq}c^2} \quad (9)$$

and

$$\epsilon = \frac{\Omega^2 R_{eq}^3}{GM} = \frac{\Omega^2 R_{eq}^2}{c^2} \frac{1}{\zeta} \quad (10)$$

with $\Omega = 2\pi/P$, where P is the spin period. The coefficients $a_n(\zeta, \epsilon)$ can then be fit to the shapes of stellar models computed using the `rns` code. The Hartle (1967) slow rotation approximation corresponds to dropping the a_4 term in the series. We find that the a_4 term is required to describe the shape of the largest, most rapidly rotating stars. However, higher order terms are not required.

We have computed the stellar structure of compact stars for a wide variety of equations of state. For each EOS, models spanning the allowed values of mass and angular velocity were computed. We find that the EOS can be grouped into two families, where each family's stars can be described by a separate set of Legendre coefficients. The first family, Neutron and Hybrid Quark Stars, includes the following EOS: Arnett & Bowers (1977) catalogue EOS A, B, C, F, G, L, N, O; EOS APR (Akmal et al. 1998) which includes nuclei scattering data and special relativistic corrections; hybrid quark stars with a mixed quark-hadron phase calculated by Alford et al. (2005); and Hyperon stars computed by Lackey, Nayyar, & Owen (2006) using methods described by Glendenning (2000). The second family consists of color-flavor-locked (CFL) quark stars described by the EOS $P = (\epsilon - 4B)/3$ where B is the bag constant. Bag constants in the range 50 – 140 MeV/fm³ are used to generate different CFL EOS. This simple EOS has been shown by Fraga et al. (2001) to be an excellent approximation to quark star models including second order perturbative QCD corrections.

Although each EOS has a different mass versus radius curves, for any given combination of mass, radius and angular velocity the scaled shape of the star is independent of the EOS within its family. The values of the Legendre fitting coefficients $a_n(\zeta, \epsilon)$ for the two families are given in Table 1. Since $R(\pi/2)$ is defined to be the equatorial radius of the rotating star, this requires that the coefficients obey $0 = a_0 - a_2/2 + 3a_4/8$. As can be seen from the coefficients in Table 1 this requirement is not exactly satisfied. However, the errors in this model are still less than 1%.

Equation (8) is only useful if the equatorial radius of the star is known. When doing light curve fits, we will need to choose a value of θ describing the spot's colatitude and the value of radius at the spot's latitude. Given these values, equation (8) can be inverted to solve for R_{eq} ,

$$\frac{R_{eq}}{R(\theta)} = 1 + \sum_{n=0}^2 b_{2n}(\tilde{\zeta}, \tilde{\epsilon}) P_{2n}(\cos \theta) + P_2(\cos \theta) \sum_{n=1}^2 c_{2n}(\tilde{\epsilon}) P_{2n}(\cos \theta), \quad (11)$$

where $\tilde{\zeta} = GM/R(\theta)c^2$ and $\tilde{\epsilon} = \Omega^2 R^3(\theta)/GM$. The values of the b_n and c_n coefficients are displayed in Table 1.

It is our intention that equation (11) be used in light curve fitting to put constraints on the equatorial radius of a rotating star. In order to compare with the predictions of a specific EOS, it is still necessary to construct a sequence of neutron stars with a specific spin frequency. The construction of such a sequence for a fixed spin frequency can be done in a straight-forward fashion using a public domain program such as `rns`.

2.2. The Normal Vector

The isotropic form of the Schwarzschild metric given in equation (4) has the useful feature that surfaces of constant time are conformally flat. This allows the introduction of quasi-Cartesian coordinates $\{x, y, z\}$ defined by $x = \bar{r} \sin \theta \cos \phi$, $y = \bar{r} \sin \theta \sin \phi$ and $z = \bar{r} \cos \theta$. In the quasi-Cartesian coordinate system the z axis is aligned with the star's spin axis, and the observer lies in the x - z plane at an angle i from the spin axis.

The vector normal to the surface at any arbitrary point can be constructed using the quasi-Cartesian coordinate system in the same way that it would be computed in flat space. First a tangent vector is constructed by taking the gradient of the function \bar{R} making use of equation (7). The normal to the surface at the location of the spot is

$$\mathbf{n} = (1 + f^2(\theta))^{-1/2} [(\sin \theta - \cos \theta f(\theta)) (\cos \phi \mathbf{x} + \sin \phi \mathbf{y}) + (\cos \theta + \sin \theta f(\theta)) \mathbf{z}]. \quad (12)$$

The unit radial vector is defined by $\mathbf{r} = \sin \theta (\cos \phi \mathbf{x} + \sin \phi \mathbf{y}) + \cos \theta \mathbf{z}$, so the angle γ between \mathbf{r} and \mathbf{n} , is simply

$$\cos \gamma = (1 + f^2(\theta))^{-1/2}. \quad (13)$$

Since $\sin \gamma = f/\sqrt{1+f^2}$, the normal vector in equation (12) can also be expressed as

$$\mathbf{n} = \sin(\theta - \gamma) (\cos \phi \mathbf{x} + \sin \phi \mathbf{y}) + \cos(\theta - \gamma) \mathbf{z} \quad (14)$$

as would be expected from simple geometric considerations in flat space.

2.3. Bending Angles and Zenith Angles

A light ray emitted in an initial direction \mathbf{l} will be moving a different direction \mathbf{k} when it reaches the observer. Since the observer is located at an angle i from the spin axis, $\mathbf{k} = \sin i \mathbf{x} + \cos i \mathbf{z}$. In the standard treatment of spherical neutron stars, α is the angle between the initial photon direction and the radial direction, defined by $\cos \alpha = \mathbf{l} \cdot \mathbf{r}$ and the bending angle ψ is defined by

$$\cos \psi = \mathbf{k} \cdot \mathbf{r} = \cos i \cos \theta + \sin i \sin \theta \cos \phi. \quad (15)$$

In the Schwarzschild metric, the vectors \mathbf{l} and \mathbf{k} are coplanar so that

$$\mathbf{l} = \frac{1}{\sin \psi} (\sin \alpha \mathbf{k} + \sin(\psi - \alpha) \mathbf{r}). \quad (16)$$

The zenith angle β between the normal vector and the initial photon direction is defined by $\cos \beta = \mathbf{l} \cdot \mathbf{n}$. Making use of equation (16), the identity $\mathbf{n} = (\sin(\theta - \gamma) \mathbf{r} + \sin \gamma \mathbf{z})/\sin \theta$, and the spherical trigonometric identity $\cos i = \cos \theta \cos \psi + \sin \theta \sin \psi \cos \delta$ (see Figure 1 for the geometrical definition of δ) the zenith angle has the value

$$\cos \beta = \mathbf{l} \cdot \mathbf{n} = \cos \alpha \cos \gamma + \sin \alpha \sin \gamma \cos \delta, \quad (17)$$

if $\sin \psi \neq 0$. If $\sin \psi = 0$, it is straight forward to show that $\cos \beta = \cos \alpha \cos \gamma$.

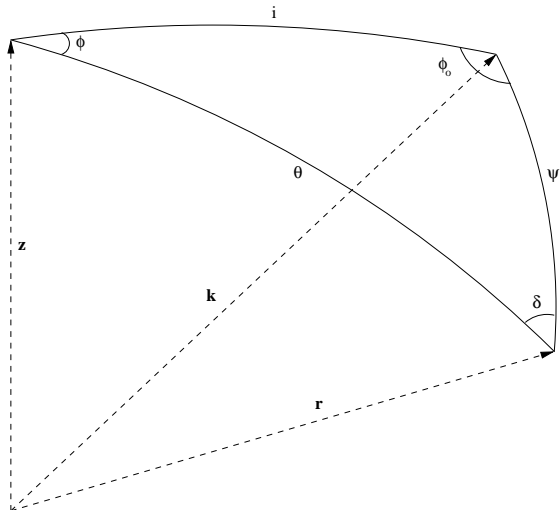


FIG. 1.— Spherical triangle illustrating the emission geometry. The vector \mathbf{z} is aligned with the spin axis, \mathbf{r} points in the direction of the spot, and \mathbf{k} points in the direction of the observer. The angles between these three vectors as well as the interior angles of the spherical triangle are shown.

2.4. Solid Angle for Static Oblate Stars

In this section we derive the solid angle subtended by a surface area element on an oblate star that is at rest. In the subsequent section we will discuss the modifications necessary when the star is rotating.

Since the photons travel to the observer via geodesics of the Schwarzschild metric, the solid angle subtended by a surface element is given by the standard expression (Pechenick, Ftaclas, & Cohen 1983)

$$d\Omega_s = \frac{b db d\phi_o}{D^2} \quad (18)$$

where b is the photon's impact parameter, D is the distance between the star and the observer, and ϕ_o is the azimuthal angle around the vector \mathbf{k} . The subscript “s” refers to static, since in this section we do not take into account Doppler shifts and boosts due to the rotation of the star. The impact parameter is related to the zenith angle α by

$$\sin \alpha = \frac{b}{R(\theta)} \sqrt{1 - \frac{2M}{R(\theta)}}. \quad (19)$$

The bending angle ψ is related to the impact parameter and the surface of the star by

$$\psi(b, R(\theta)) = b \int_{R(\theta)}^{\infty} \frac{dr}{r^2} \left(1 - \frac{b^2}{r^2} \left(1 - \frac{2M}{r} \right) \right)^{-1/2}. \quad (20)$$

In order to express the solid angle in terms of the coordinates defined on the surface of the star, a change of variables from coordinates $\{b, \phi_o\}$ to $\{\psi, \phi_o\}$ must be made so that

$$d\Omega_s = \left(\frac{\partial b}{\partial \psi} \right)_{\phi_o} \frac{b d\psi d\phi_o}{D^2}. \quad (21)$$

The relationship between the impact parameter and the bending angle for a spherical star is simple, since the photons are emitted from a surface of constant gravitational potential. In the case of an oblate star, the bending angle

ψ depends on both the impact parameter and the variable location of the star's surface. The partial derivative appearing in equation (21) is

$$\left(\frac{\partial b}{\partial \psi} \right)_{\phi_o} = \left(\frac{\partial b}{\partial \psi} \right)_R + \left(\frac{\partial b}{\partial R} \right)_\psi \left(\frac{\partial R}{\partial \psi} \right)_{\phi_o} \quad (22)$$

where $(\partial b / \partial \psi)_R = 1 / (\partial \psi / \partial b)_R$ is evaluated using the integral definition given in equation (20). Making use of standard relations for partial derivatives

$$\left(\frac{\partial b}{\partial R} \right)_\psi = - \left(\frac{\partial b}{\partial \psi} \right)_R \left(\frac{\partial \psi}{\partial R} \right)_b. \quad (23)$$

Using equations (19) and (20) the second partial derivative appearing on the right-hand side of equation (23) is

$$\left(\frac{\partial \psi}{\partial R} \right)_b = - \frac{(1+z) \sin \alpha}{R \cos \alpha}. \quad (24)$$

The partial derivative of R with respect to ψ can be calculated using equations (3) and (13),

$$\frac{1}{R} \left(\frac{\partial R}{\partial \psi} \right)_{\phi_o} = - \frac{f(\theta)}{(1+z) \sin \theta} \left(\frac{\partial \cos \theta}{\partial \psi} \right)_{\phi_o}. \quad (25)$$

Making use of standard identities for the spherical triangle defined in Figure 1,

$$\left(\frac{\partial \cos \theta}{\partial \psi} \right)_{\phi_o} = - \sin \theta \cos \delta. \quad (26)$$

The $\cos \delta$ term in this last expression can be eliminated using equation (17), leading to the simple equation

$$\frac{1}{R} \left(\frac{\partial R}{\partial \psi} \right)_{\phi_o} = \frac{(\cos \beta - \cos \alpha \cos \gamma)}{(1+z) \cos \gamma \sin \alpha}. \quad (27)$$

The final result for equation (22) is

$$\left(\frac{\partial b}{\partial \psi} \right)_{\phi_o} = \left(\frac{\partial b}{\partial \psi} \right)_R \cos \beta. \quad (28)$$

The expression for the solid angle can now be simplified to

$$d\Omega_s = (1+z)^2 \frac{R^2}{D^2} \cos \beta \left| \frac{\partial \cos \alpha}{\partial \cos \psi} \right|_{\phi_o} \frac{\sin \psi}{\cos \gamma} d\psi d\phi_o. \quad (29)$$

The transformation between the $\{\psi, \phi_o\}$ coordinates to the star's coordinates $\{\theta, \phi\}$ is given by the usual relation $\sin \psi d\psi d\phi_o = \sin \theta d\theta d\phi$. Equation (2) can now be used to simplify the solid angle formula to

$$d\Omega_s = (1+z)^2 \frac{dS}{D^2} \cos \beta \left| \frac{\partial \cos \alpha}{\partial \cos \psi} \right|_{\phi_o}. \quad (30)$$

The solid angle subtended by a spot on an oblate star given by equation (30) is very similar to the expression for the solid angle subtended by a spot on a spherical surface. The expressions for the oblate and spherical surfaces differ through the $\cos \beta$ term, corresponding to the cosine of the angle between the initial photon direction and the vector normal to the surface. In the spherical case, $\cos \beta$ is replaced by $\cos \alpha$, the cosine of the angle between the initial photon direction and the radial vector. Hence our result for the solid angle reduces to a simple correction for the tilt of the surface induced by oblateness.

3. LIGHT CURVES FOR ROTATING OBLATE STARS

The flux due to a spot on the star is

$$dF = I_o d\Omega_o \quad (31)$$

where I_o is specific intensity measured in the observer's frame and $d\Omega_o$ is the solid angle subtended by the spot as measured by the observer.

Light emitted with frequency ν_{em} will be detected with frequency ν_o given by

$$\nu_o = \frac{\eta}{1+z} \nu_{em} \quad (32)$$

where η is the Doppler boost factor given by

$$\eta = \frac{\sqrt{1-v^2}}{1-v \cos \xi}, \quad (33)$$

where v is the magnitude of the spot's velocity and ξ is the angle between the velocity and the original photon direction. The spot's velocity is unaffected by the oblate shape of the star, so the functions v and ξ are given by the values

$$v = 2\pi\nu_* R(\theta) \sin \theta \left(1 - \frac{2M}{R}\right)^{-1/2} \quad (34)$$

and

$$\cos \xi = -\frac{\sin \alpha \sin i \sin \phi}{\sin \psi}. \quad (35)$$

The motion of the spot causes an aberration in the angles between the normal to the surface and the initial photon direction as measured in the rest frame of the spot, β_{em} and the observer at infinity, β , given by

$$\cos \beta_{em} = \eta \cos \beta \quad (36)$$

where β is given by equation (17). In order for the spot to be visible, it is necessary that $0 \leq \cos \beta_{em} \leq 1$. The solid angle measured at infinity $d\Omega_o$ is also affected by the spot's motion, and is related to the solid angle derived in the previous section by

$$d\Omega_o = \eta d\Omega_s. \quad (37)$$

A photon emitted from $R(\theta)$ and with impact parameter b will arrive at a time

$$T(b, R(\theta)) = \int_{R(\theta)}^{\infty} dr \left(1 - \frac{2M}{r}\right)^{-1} \times \left(\left(1 - \frac{b^2}{r^2} \left(1 - \frac{2M}{r}\right)\right)^{-1/2} - 1 \right) \quad (38)$$

relative to a photon with zero impact parameter emitted from the same location.

Finally, making use of the relativistic conservation law $I_o/\nu_o^3 = I/\nu_{em}^3$, the measured flux is

$$F_{\nu_o} = \int_{\cos \beta_{em} > 0} d\Omega_s \eta^4 (1+z)^{-3} I(\cos \beta_{em}, \nu_{em}) \quad (39)$$

where $d\Omega_s$ is given by equation (30). In order to produce a light curve the flux should be integrated over the observed frequency range, and the flux should be binned according to the relative arrival times of the photons. Times of arrival can be computed exactly using equation (38) or a series expansion such as that given by Poutanen & Beloborodov (2006) (see their equation 18) can be used.

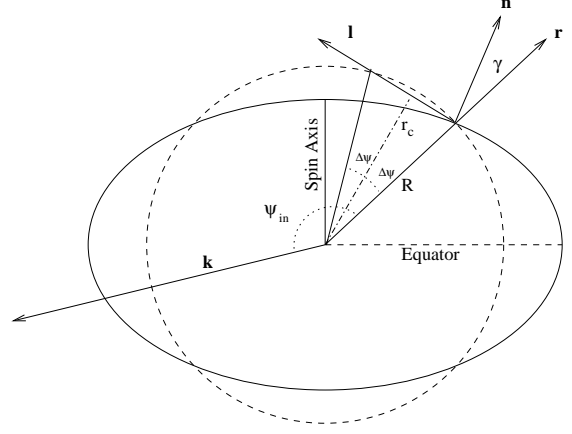


FIG. 2.— Side view of a rotating neutron star (solid curve). The surface of a spherical star with the same radius as the oblate star at the emission latitude is shown as a dashed circle. A photon with initial direction \mathbf{l} is initially moving towards smaller values of the radial coordinate. At r_c the photon reaches the minimum value of r and begins to move outwards. The change in bending angle while the photon travels between the two intersections of the solid and dashed curves is $2\Delta\psi$.

3.1. Initially Ingoing Photons

For photons that are emitted in an outgoing direction, the calculation of the flux is straightforward and similar to the standard calculation for a star with a spherical surface. However, because the surface is oblate, there will be photons emitted which are initially directed radially inwards. These photons will travel to smaller values of r until a critical radial coordinate r_c is reached, at which point $\dot{r} = 0$. After the critical radius has been reached, the photon will move outwards. In Figure 2 an initially ingoing photon's trajectory is labelled by vector \mathbf{l} .

An initially ingoing photon will have a value of impact parameter

$$b_{in} \leq \frac{R}{\sqrt{1-2M/R}}, \quad (40)$$

and an angle $\alpha > \pi/2$. The quantity R is the location of the surface of the star at the latitude of the spot. The critical radius is given by the solution of the equation

$$r_c = b_{in} \sqrt{1 - \frac{2M}{r_c}}. \quad (41)$$

Given this critical radius, the bending angle associated with the motion of the photon from R to r_c is $\Delta\psi$ given by the integral

$$\Delta\psi = b_{in} \int_{r_c}^R \frac{dr}{r^2} \left(1 - \frac{b_{in}^2}{r^2} \left(1 - \frac{2M}{r}\right)\right)^{-1/2}. \quad (42)$$

Similarly, the relative coordinate time taken by the photon to travel this distance is

$$\Delta T = \int_{r_c}^R dr \left(1 - \frac{2M}{r}\right)^{-1} \left(1 - \frac{b_{in}^2}{r^2} \left(1 - \frac{2M}{r}\right)\right)^{-1/2} \quad (43)$$

By symmetry, when the photon travels from r_c out to R the bending angle is $\Delta\psi$ and the extra time is ΔT . The final result is that the total bending angle for an initially ingoing photon is

$$\psi_{in}(b_{in}, R) = 2\Delta\psi + \psi(b_{in}, R) \quad (44)$$

where $\psi(b, R)$ is given by equation (20). Similarly, the relative arrival time for the photon is

$$T_{in}(b_{in}, R) = 2\Delta T + T(b_{in}, R). \quad (45)$$

As expected, an initially ingoing photon will have a larger bending angle and take longer to reach the observer than an initially outgoing photon with the same value of impact parameter.

In all situations of interest, the difference $R(\theta) - r_c$ will always be much smaller than the radius of the star. This makes it possible to approximate the integrals $\Delta\psi$ and ΔT by assuming that in the integrand $r = r_c(1 + \varepsilon)$ where $\varepsilon \ll 1$. To lowest order in $\varepsilon^{1/2}$,

$$\Delta\psi = \sqrt{2 \frac{(R - r_c)}{(r_c - 3M)}}. \quad (46)$$

Similarly an approximation for ΔT is

$$\Delta T = r_c(1 - 2M/r_c)^{-1/2} \Delta\psi. \quad (47)$$

4. EFFECT OF OBLATENESS ON LIGHT CURVES

It may seem counter-intuitive that the oblateness of a rotating star could have an important effect on the resulting light curves since a naive argument predicts that oblateness is unimportant: since oblateness is an effect that is second-order in angular velocity it ought to be smaller than first-order effects such as Doppler effects and the frame-dragging effect. However, Cadeau et al. (2007) have shown that the effect of oblateness can be large in some cases. The main reason why oblateness can't be neglected is *not* through its effect on the star's gravitational field. It is instead a simpler geometric argument that would also hold in flat space. We now explain why the naive argument fails for certain ranges of spot locations.

Doppler shifts and boosts are first-order corrections to the shape of a light curve, so Doppler corrections are the most important effect. As has been shown elsewhere (for example Poutanen & Gierliński (2003)) Doppler boosting creates an asymmetry in the light curve. However, Doppler effects are most important when the spot is moving in the same direction as the initial photon direction. For light emitted near the back of the star (for values of rotational phase near $\phi = \pi$) the angle ξ defined in equation (35) is close to $\pi/2$ so that the boost factor in equation (33) only differs from unity by corrections that are second order in v/c . It is in this region near the back of the star that oblateness effects become most important.

Frame-dragging is almost always a more significant contribution to the gravitational field than the contributions to the field due to oblateness. Only at very high spin frequencies when $\epsilon \sim 0.1$ (corresponding to about 500 Hz, depending on the EOS) do the oblateness corrections to the spacetime metric become comparable to the frame-dragging corrections. However, neither correction has a strong influence on the trajectories of photons or the resulting light curves. As the photon moves away from the star, the frame-dragging frequency falls off as r^{-3} so it rapidly becomes unimportant. (Corrections due to oblateness fall off even faster.) In our previous calculations (Cadeau et al. 2007) we found very little difference between the light curves computed with the Kerr or

Schwarzschild metric. For this reason, the use of the Kerr metric (which keeps the frame-dragging term in the metric) is not a great improvement over the Schwarzschild metric (which ignores frame-dragging) when computing light curves.

Oblateness affects lights curves in two ways: the solid angle is changed since the emitting surface is tilted at a different angle with respect to the initial photon direction; and the visibility condition is altered. The first effect is usually small (except near the back of the star) while the second effect can be surprisingly large.

The first oblateness effect is easily seen in equation (30) for the solid angle of an oblate star. This expression is equivalent to the expression for the solid angle of a spherical star multiplied by the factor $\cos\beta/\cos\alpha$. This factor corrects for the change in the tilt of the surface due to oblateness. Since $\cos\beta$ (the angle between the surface normal and the initial photon) only differs from $\cos\alpha$ (the angle between the radial direction and the initial photon) by an amount of order $\mathcal{O}(\Omega^2)$ this correction is not typically large. However, near the back of the star (in relation to the observer) this correction factor can be important if $\cos\alpha$ is of similar order of magnitude as γ or smaller. In order to see this, consider the value of phase $\phi = \pi$, corresponding to the back of the star. At this point, equation (17) for the zenith angle reduces to $\cos\beta = \cos\alpha \cos\gamma + \sin\alpha \sin\gamma$. If $\cos\alpha$ is small and $\mathcal{O}(\cos\alpha) \sim \mathcal{O}(\gamma)$ then $\cos\beta/\cos\alpha \sim 1 + \gamma/\cos\alpha + \mathcal{O}(\gamma^2)$. In this case the correction factor $\cos\beta/\cos\alpha$ is not necessarily close to unity, and can cause large changes in the received flux. Similar arguments hold for other values of phase as long as $\cos\alpha$ is small.

The second effect of oblateness, due to the change in the visibility condition, can be understood with a simple example. Consider a spot at fixed latitude θ on two equal-mass stars, a spherical star and an oblate star, chosen so that the radii of the two stars at the spots' latitude are the same. Suppose that at the value of rotational phase denoted ϕ_1 the spot is at the limb of the spherical star. This means that $\alpha = \pi/2$ and the bending angle is at its maximum value, ψ_{max} . Using equation (15) $\cos\psi_{max} = \cos i \cos\theta + \sin i \sin\theta \cos\phi_1$.

Similarly, on the oblate star, the spot is at the limb at rotational phase $\phi_2 = \phi_1 + \Delta\phi$ at which point $\beta = \pi/2$ and the angle between the radial direction and the initial photon direction is α_2 , differing by $\pi/2$ by an amount second order in angular velocity. The bending angle for light emitted from ϕ_2 is $\cos\psi_2 = \cos i \cos\theta + \sin i \sin\theta \cos\phi_2$. The difference between the rotational phases on the two stars where the spot is at the limb is given by

$$\cos\phi_2 - \cos\phi_1 = \frac{\cos\psi_2 - \cos\psi_{max}}{\sin i \sin\theta} = \left(\frac{d \cos\psi}{d \cos\alpha} \right)_{\alpha_2} \frac{\cos\alpha_2}{\sin i \sin\theta}. \quad (48)$$

If we assume that the phase difference, $\Delta\phi$ is very small, and that the spot is very close to the back of the star so that $\phi_1 \sim \pi$, then $\cos\phi_2 - \cos\phi_1 = (\Delta\phi)^2/2$. As a result, the change of phase over which the spot is visible due to oblateness is approximately

$$\Delta\phi \sim \left(\frac{2}{\sin i \sin\theta} \left(\frac{d \cos\psi}{d \cos\alpha} \right)_{\alpha_2} \cos\alpha_2 \right)^{1/2} \quad (49)$$

when the spot is near the back of the star. In the Beloborodov (2002) approximation $d \cos\psi/d \cos\alpha \sim (1 +$

$z)^2$ for light emitted close to the normal to the surface. In our example light is emitted close to the tangent to the surface, but the cosine derivative continues to be finite and order unity. Since $\cos \alpha_2 \sim \mathcal{O}(\Omega^2)$ it follows that the phase difference $\Delta\phi \sim \mathcal{O}(\Omega)$. As a result, for light emitted on the side of the star opposite the observer, the phase differences caused by oblateness are first order in the angular velocity. Since the Doppler boosting is only second order in the angular velocity in this region of the star, oblateness becomes the dominant effect.

5. COMPARISON OF MODELS

The effect of oblateness is most important for very large neutron stars rotating with very high spin frequencies. In order to test the accuracy of the OS approximation discussed in this paper, we now examine the results of this approximation for one very oblate neutron star with a mass of $1.4M_\odot$, an equatorial radius of $R_{eq} = 16.4$ km and a spin frequency of 600 Hz. The expansion parameters defined in equations (9) and (10) take on values of $\zeta = 0.126$ and $\epsilon = 0.339$ for this model.

Consider first the case of emission from a spot at co-latitude $\theta = 49^\circ$. The radius of the star (computed using the exact numerical method) at this point is $R(\theta) = 15.1$ km. The oblateness model given by equation (8) differs from this value only in the fourth significant figure. In Figure 3 light curves for light emitted from this co-latitude and observed at an inclination of $i = 70^\circ$ are shown. The bold solid curve labelled “exact” is computed using the exact numerical method described by Cadeau et al. (2007). The curve labelled “S+D” is computed for a spherical $1.4M_\odot$ star with a radius of 15.1 km. The curve labelled “OS” is computed using the Oblate Schwarzschild approximation described in this paper. For this combination of emission and observer angles, the S+D approximation predicts an eclipse for part of the rotational period. In the cases of the exact calculation and the OS approximation the spot is visible all of the time. The small differences between the Exact and OS light curves are due to differences in the spacetime metric and to small errors due to the oblateness model given in equation (8). The differences between the OS and Exact light curves are very small compared to the differences between the S+D and Exact light curves.

In Figure 4 light curves for the same star are shown, but in this case light is emitted from a co-latitude of $\theta = 41^\circ$, and the observer’s inclination is $i = 20^\circ$. For this stellar model, the radius of the star at $\theta = 41^\circ$ is 14.8 km. The light curves in Figure 4 have the same meaning as in the previous figure, however for the S+D approximation, the surface of the spherical star is chosen to be 14.8 km, in order to keep the values of the gravitational potentials the same in both OS and S+D approximations. As in the case for emission from 49° , the OS and Exact light curves differ by an amount which is much smaller than the difference between the S+D and the Exact light curves.

6. CONCLUSIONS

In our previous work (Cadeau et al. 2007) we demonstrated the need to include the oblateness of rapidly rotating neutron star when computing light curves. In this paper we presented a simple method, the Oblate Schwarzschild approximation which can be used to ac-

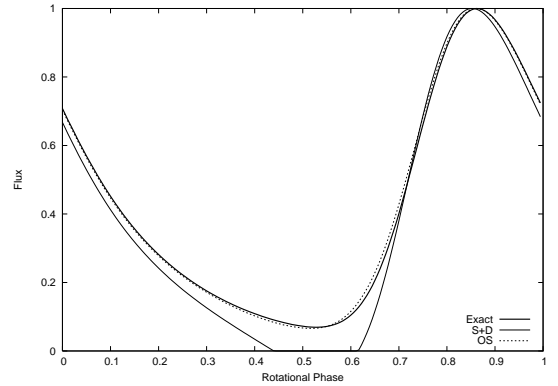


FIG. 3.— Light curves for light emitted from a co-latitude of $\theta = 49^\circ$ and an observer at an inclination of $i = 70^\circ$. The neutron star has $M = 1.4M_\odot$, $R_{eq} = 16.4$ km and spins at 600 Hz. The solid bold curve is computed using the exact numerical space time, as described by Cadeau et al. (2007). The solid curve labelled S+D is computed by assuming that the star’s surface is spherical. The dashed curve is computed using the Oblate Schwarzschild approximation described in this paper.

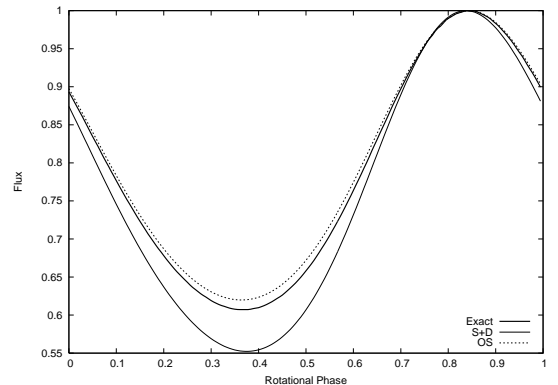


FIG. 4.— Light curves for light emitted from a co-latitude of $\theta = 41^\circ$ and an observer at an inclination of $i = 20^\circ$. The neutron star’s parameters are exactly as given in Figure 3.

count for the star’s oblate shape. The method presented in sections 2 and 3 can be summarized as follows. First the mass, radius and angular velocity of the neutron star are chosen. The shape of the star’s surface is then given by the empirical formula given in equation (8), which in turn allows the calculation of the angles γ and β , where γ is the angle between the surface normal and the radial direction, and β is the angle between the initial photon direction and the surface normal. Given the angle β , the light curve for the rapidly rotating neutron star can be computed using the same formulae used in the S+D approximation (as given, for example by Poutanen & Gierliński (2003)) with the following changes: the angle α (between the initial photon direction and the radial direction) is replaced by β ; the visibility condition is given by $0 \leq \cos \beta \leq 1$; and the photons must be binned by their times of arrival. In the OS approximation the bending angles and times of arrival are calculated using the Schwarzschild metric. The resulting light curves closely approximate the exact light curves, as shown in section 5.

The accreting ms X-ray pulsars such as SAX J1808.4-3658 (Wijnands & van der Klis 1998;

TABLE 1
NEUTRON STAR SHAPE PARAMETERS

Coefficient	Neutron and Hybrid Quark Stars	CFL Quark Stars
a_0	$-0.18\epsilon + 0.23\zeta\epsilon - 0.05\epsilon^2$	$-0.26\epsilon + 0.50\zeta\epsilon - 0.04\epsilon^2$
a_2	$-0.39\epsilon + 0.29\zeta\epsilon + 0.13\epsilon^2$	$-0.53\epsilon + 0.85\zeta\epsilon + 0.06\epsilon^2$
a_4	$+0.04\epsilon - 0.15\zeta\epsilon + 0.07\epsilon^2$	$+0.02\epsilon - 0.14\zeta\epsilon + 0.09\epsilon^2$
b_0	$+0.18\bar{\epsilon} - 0.23\zeta\bar{\epsilon} + 0.18\bar{\epsilon}^2$	$+0.26\bar{\epsilon} - 0.50\zeta\bar{\epsilon} + 0.31\bar{\epsilon}^2$
b_2	$+0.39\bar{\epsilon} - 0.29\zeta\bar{\epsilon} + 0.42\bar{\epsilon}^2$	$+0.53\bar{\epsilon} - 0.85\zeta\bar{\epsilon} + 1.06\bar{\epsilon}^2$
b_4	$-0.04\bar{\epsilon} + 0.15\zeta\bar{\epsilon} - 0.13\bar{\epsilon}^2$	$-0.02\bar{\epsilon} + 0.14\zeta\bar{\epsilon} - 0.12\bar{\epsilon}^2$
c_2	$+0.60\bar{\epsilon}^2$	$+1.13\bar{\epsilon}^2$
c_4	$-0.12\bar{\epsilon}^2$	$-0.07\bar{\epsilon}^2$

Chakrabarty & Morgan 1998) are rotating rapidly enough that light curve models should include the oblateness model presented in this paper along with realistic models of the emission spectrum and geometry. Comparisons of the light curves arising from these oblate models with data for SAX J1808.4-3658 are currently in progress (Leahy et al. 2007).

This research was supported by grants from NSERC. We thank Mark Alford and Ben Owen for providing us with equation of state files. S. M. M. thanks the Pacific Institute for Theoretical Physics and the Department of Physics & Astronomy at the University of British Columbia for hospitality during her sabbatical.

REFERENCES

- Alford, M., Braby, M., Paris, M., & Reddy, S. 2005, *ApJ* 629, 969
Akmal, A., Pandharipande, V. R., & Ravenhall, D. G. 1998, *Phys. Rev. C*, 58, 1804
Arnett, W. D., & Bowers, R. L. 1977, *ApJS*, 33, 415
Beloborodov, A. M. 2002, *ApJ*, 566, L85
Bhattacharyya, S., Strohmayer, T. E., Miller, M. C., & Markwardt, C. B. 2005, *ApJ*, 619, 483
Bogdanov, S., Rybicki, G. B., & Grindlay, J. E. 2006, *arXiv:astro-ph/0612791*
Braje, T. M., & Romani, R. W. 2001, *ApJ*, 550, 392
Braje, T. M., Romani, R. W., & Rauch, K. P. 2000, *ApJ*, 531, 447
Cadeau, C., Leahy, D. A., & Morsink, S. M. 2005, *ApJ*, 618, 451
Cadeau, C., Morsink, S. M., Leahy, D. A., & Campbell, S. S. 2007, *ApJ*, 654, 458
Chakrabarty, D., & Morgan, E. H. 1998, *Nature*, 394, 346
Cook, G. B., Shapiro, S. L., Teukolsky, S. A. 1994, *ApJ*, 424, 823
Fraga, E. S., Pisarski, R. D., & Schaffner-Bielich, J. 2001, *Phys. Rev. D*, 63, 121702
Glendenning, N. K. 2000, *Compact Stars*, (Springer-Verlag, New York).
Hartle, J. 1967, *ApJ* 150, 1005
Lackey, B. D., Nayyar, M., & Owen, B. J. 2006, *Phys. Rev. D*, 73, 024021
Leahy, D. A. 2004, *ApJ*, 613, 517
Leahy, D. A., Morsink, S. M., & Cadeau, C. 2007, submitted to *ApJ*, *astro-ph/0703287*
Miller, M. C. & Lamb, F. K. 1998, *ApJ*, 499, L37
Misner, C. W., Thorne, K. S., & Wheeler, J. A. 1973, *Gravitation*, W.H. Freeman and Co.
Pechenick, K. R., Ftacilas, C., & Cohen, J. M. 1983, *ApJ*, 274, 846
Poutanen, J., & Beloborodov, A. M. 2006, *MNRAS*, 373, 836
Poutanen, J. & Gierliński, M. 2003, *MNRAS*, 343, 1301
Stergioulas, N. & Friedman, J. L. 1995, *ApJ*, 444, 306
Wijnands, R., & van der Klis, M. 1998, *Nature*, 394, 344